Detectability of deep conductive anomaly for geothermal exploration by 3D FEM and FDM inversions of MT data

Toshihiro Uchida and Yusuke Yamaya
Geothermal Energy Team, National Institute of Advanced Industrial Science and Technology,
toshi2travel@gmail.com

Summary

We performed numerical experiments to investigate how accurately we can detect a deep conductive anomaly which is overlain by another shallow conductive layer. Baring in mind the exploration of geothermal reservoirs, real topography data from a field survey was considered in the experiment. We utilized two three-dimensional magnetotelluric inversion codes; FEMTIC (finite element modeling; FEM) and WSINV3DMT (finite difference modeling; FDM). For FEMTIC, we also tested the inclusion of phase tensor as observed data. Inversion experiments revealed the following; 1) the FEM inversion can almost properly recover both the shallow and deep conductive anomalies with the inversion of impedance and tipper data, 2) Inclusion of phase tensor data, instead of the impedance data, may lose the detectability of the deep conductor, and 3) the FDM inversion is not accurate to recover the deep conductive anomaly when we include rough topography variation.

Keywords: magnetotellurics, 3D inversion, deep conductive anomaly, topography, geothermal

Introduction

We often observe a deep low-resistivity anomaly beneath a geothermal reservoir in an electrical model obtained by three-dimensional (3D) inversion of magnetotelluric (MT) data. This anomaly may be related to the heat source of the geothermal system. However, it may also be an artifact caused by inaccurate inversion or strong noises in low-frequency observed data. In this study, we carried out a numerical experiment to investigate how accurately the deep anomaly can be recovered by the inversion. We used two 3D MT inversion codes; FEMTIC that uses the finite-element modeling scheme (Usui, 2015; Usui et al., 2017), and WSINV3DMT that utilizes the finite-difference method (Siripunvaraporn and Egbert, 2009).

Method

The 3D synthetic model in this study contains two conductive anomalies embedded in a homogeneous earth of 100 ohm-m; one represents a shalow low-resistivity cap rock (5 ohm-m) and the other represents a deep conductive anomaly (1 ohm-m). Location of MT stations was based on a field survey conducted in the Okuaizu geothermal field, northern Japan (Uchida et al., 2015) and the real topography was included in the model.

Figure 1 shows bird-eye views of the mesh for FEMTIC and WSINV3DMT modeling. We used the deformed non-conforming hexahedral elements (DHexa) for FEMTIC. For the DHexa mesh, the size of hexahedral elements near MT stations was about 30 m horizontally and 25 m vertically, and it became larger as we moved away from the MT stations. For WSINV3DMT, the size of rectangular cells near the surface was 150 m horizontally and 10 m vertically in the survey area where MT stations were deployed.

The number of MT stations was 58, of which 46 stations in the central zone were deployed as a grid-like array. All components of the impedance and tipper at 16 frequencies (0.00275 – 97 Hz) were used in the experiment. Phase tensor was also used as observed data in the FEMTIC inversion. Elevation of MT stations spans from 330 m to 720 m above sea level.

Figure 2a shows the synthetic model to generate numerical dataset by the FEMTIC code, while Figure 3a shows the model for the WSINV3DMT code. For WSINV3DMT, the size of the shallow conductive anomaly (5 ohm-m) was 4950 m in the x direction (north-south), 5100 m in the y direction (east-west), and 275 m in the vertical direction, centered at x=1450 m, y=0 m and z=37.5 m (downward positive). The size of the deep conductive anomaly (1 ohm-m) was 1950 m in the x direction, 2100 m in the y direction, and 2771 m in the vertical direction, centered at x=525 m, y=0 m, z=2872 m. The sizes of two anomalies are similar for the FEMTIC model, but slightly different from

WSINV3DMT because of the difference of the mesh setting. Forward responses from these two models were used as synthetic observed data for further inversions. Gaussian random noises were added to the responses; standard deviation of 2% to off-diagonal components of impedance, 4% to diagonal components, and 0.01 to tipper. Noise floors for the inversion were 1%, 2% and 0.005 for off-diagonal, diagonal and tipper components, respectively.

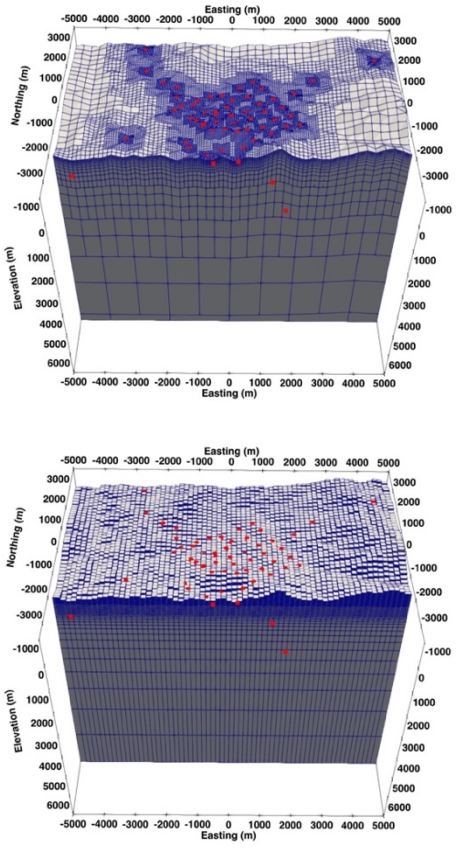

Figure 1. Mesh setting for the survey area; a) FEMTIC DHexa and b) WSINV3DMT. Red dots indicate MT stations.

Experiment results

Figure 2b shows the result of the inversion of impedance and tipper data generated from the model shown in Figure 2a, while Figure 2c shows the inversion of phase tensor and tipper data. Regarding the shallow anomaly, its shape and resistivity value were almost properly recovered by both cases, although the boundary became slightly dim. Northern extent of the anomaly was also detected properly, although there are no MT stations nearby. On the other hand, the deep anomaly was more properly recovered by the impedance-and-tipper inversion, while the phase-tensor-and-tipper inversion shows less clear conductive anomaly.

Figure 2d shows the model by the inversion of impedance-and-tipper data using only 46 stations in the central zone. The model is similar to the one by the 58-station inversion (Figure 2b). Surprisingly, the northern boundary of the shallow anomaly was also recovered. It means that the data in the central zone have the effect of the northern boundary, which is about 2 km north from the MT stations.

Figure 3b shows the result of the WSINV3DMT inversion using the synthetic data generated from the model shown in Figure 3a. The final RMS misfit is larger than those by the FEMTIC inversions (Figure 2). Shape of the shallow anomaly is not so clear, both horizontal and vertical directions, when we compare it with the FEMTIC inversion (Figure 2b). The deep anomaly is not clearly recovered either.

Discussions

The following points are observed by the numerical experiments.

- The forward modeling by the FEMTIC code including the topography seems to be accurate enough. Inversion of the impedance-and-tipper data almost properly recovers the true model. On the other hand, the inversion of the phase-tensor-and-tipper data loses the detectability of the deep conductive anomaly, probably because the amplitude information of the impedance is needed to detect the deep anomaly overlain by a shallow low-resistivity layer.
- The FEMTIC inversion is able to recover a resistivity boundary up to a long distance outside of the MT station coverage.
- The forward modeling by the WSINV3DMT code including the topography is not accurate enough. Numerical errors in the computation of MT responses and the Jacobian matrix may affect the accuracy of the inversion when rough topography is included.

References

Siripunvaraporn, W., Egbert, G. (2009) WSINV3DMT: Vertical magnetic field transfer function inversion and parallel implementation. Physics of the Earth and Planetary Interiors, 173, 317-329. doi:10.1016/j.pepi.2009.01.013.

Uchida, T., Takakura, S., Ueda, T., Sato, T., Abe, Y. (2015) Three-Dimensional Resistivity Structure of the Yanaizu-Nishiyama Geothermal Reservoir, Northern Japan. Proceedings of World Geothermal Congress 2015, Melbourne, Australia, 7p.

Usui, Y. (2015) 3-D inversion of magnetotelluric data using unstructured tetrahedral elements: applicability to data affected by topography. Geophys. J. Int., 202, 828-849. doi:10.1093/gji/ggv186.

Usui, Y., Ogawa, Y., Aizawa, K., Kanda, W., Hashimoto, T., Koyama, T., Yamaya, Y., Kagiyama, T. (2017) Three-dimensional resistivity structure of Asama Volcano revealed by data-space magnetotelluric inversion using unstructured tetrahedral elements. Geophys. J. Int., 208, 1359-1372. doi:10.1093/gji/ggw459.

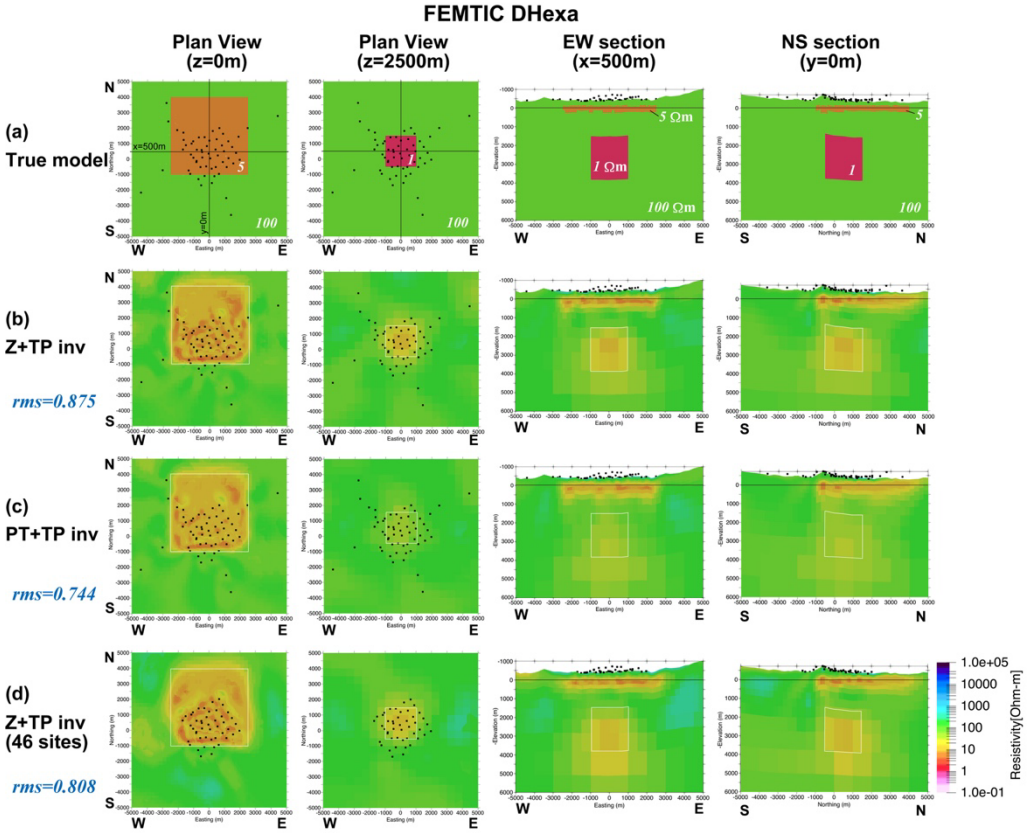

Figure 2. Numerical experiment of 3D MT inversion using the FEMTIC code; a) synthetic model used to generate numerical dataset for the inversion, b) inversion result of the impedance-and-tipper data, c) inversion result of the phase-tensor-and-tipper data, and d) inversion result of the impedance-and-tipper data from 46 MT stations in the central zone. Black dots are MT stations. White rectangles in panels b), c) and d) are boundaries of the anomalies shown in panel a). “rms” on the left means the final RMS misfit.

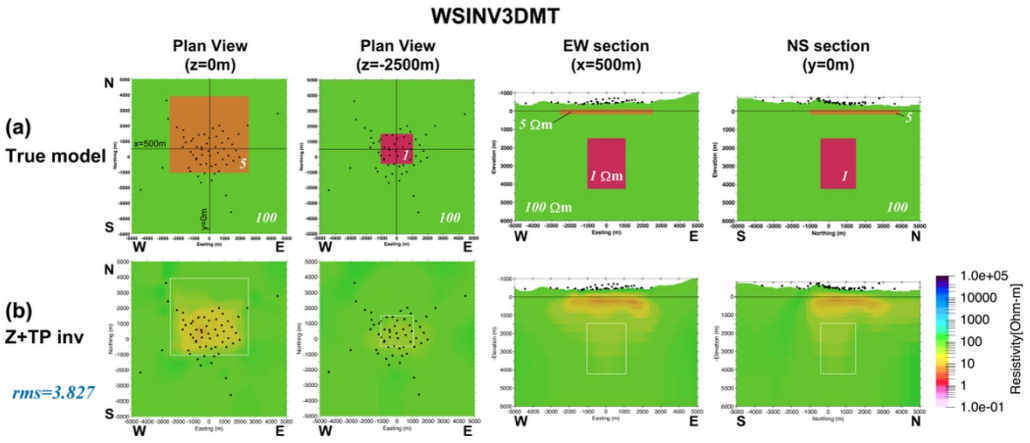

Figure 3. Numerical experiment of 3D MT inversion using the WSINV3DMT code: a) synthetic model used to generate numerical dataset for the inversion, and b) inversion result of the impedance-and-tipper data. Black dots are MT stations. White rectangles in panel b) are boundaries of the anomalies shown in panel a).